



# **Synthesis and Research of Nanocompositions of Oxide Materials Based on Titanium Dioxide for use as Contrast Agents in Optical Coherence Tomography**

**Artem Nikolaevich Kupriyanov<sup>1</sup>, Diana Evgen'evna Fidarova<sup>2</sup>,  
Linda Ruslanovna Makhmudova<sup>3</sup>, Magomed Rasulovich Gadzhiev<sup>4</sup>,  
Shuainat Ruslanovna Nimatulaeva<sup>4</sup>, Magomed Narimanovich Durniyazov<sup>4</sup>,  
Alina Yuryevna Maslova<sup>1</sup> and Sergey Nikolaevich Povetkin<sup>5\*</sup>**

<sup>1</sup>*Stavropol State Medical University, Stavropol, Russia.*

<sup>2</sup>*North Ossetian State University (Named After K. L. Khetagurov), Vladikavkaz,  
Republic of North Ossetia, Russia.*

<sup>3</sup>*Medical Institute of the Chechen State University, Grozny, Chechen Republic, Russia.*

<sup>4</sup>*Dagestan State Medical University, Dagestan, Russia.*

<sup>5</sup>*North Caucasus Federal University, Stavropol, Russia.*

## **Authors' contributions**

*This work was carried out in collaboration among all authors. All authors read and approved the final manuscript.*

## **Article Information**

DOI: 10.9734/JPRI/2021/v33i40A32252

### Editor(s):

(1) Dr. Paola Angelini, University of Perugia, Italy.

### Reviewers:

(1) M. Muhamed Haneefa, AMET University, India.

(2) C. Karthik, St. Joseph's College of Engineering, India.

Complete Peer review History: <https://www.sdiarticle4.com/review-history/71918>

**Original Research Article**

**Received 01 June 2021**

**Accepted 06 August 2021**

**Published 07 August 2021**

## **ABSTRACT**

In this paper, the contrasting properties of titanium dioxide nanoparticles in various compositions were considered. In the course of the work, methods for the synthesis of oxide materials SiO<sub>2</sub>-TiO<sub>2</sub>, SiO<sub>2</sub>-ZrO<sub>2</sub>, TiO<sub>2</sub>-ZrO<sub>2</sub> and SiO<sub>2</sub>-TiO<sub>2</sub>-ZrO<sub>2</sub> were developed; the microstructure of oxide materials SiO<sub>2</sub>-TiO<sub>2</sub>, SiO<sub>2</sub>-ZrO<sub>2</sub>, TiO<sub>2</sub>-ZrO<sub>2</sub> and SiO<sub>2</sub>-TiO<sub>2</sub>-ZrO<sub>2</sub> was studied; the stability of oxide materials SiO<sub>2</sub>-TiO<sub>2</sub>, SiO<sub>2</sub>-ZrO<sub>2</sub>, TiO<sub>2</sub>-ZrO<sub>2</sub> and SiO<sub>2</sub>-TiO<sub>2</sub>-ZrO<sub>2</sub> was determined. The elemental composition of the oxide materials SiO<sub>2</sub>-TiO<sub>2</sub>, SiO<sub>2</sub>-ZrO<sub>2</sub>, TiO<sub>2</sub>-ZrO<sub>2</sub> and SiO<sub>2</sub>-TiO<sub>2</sub>-ZrO<sub>2</sub> has also been studied

using SEM and XRD methods. It was found that  $\text{SiO}_2\text{-TiO}_2\text{-ZrO}_2$  nanocomposites with content of titanium dioxide from 8 to 9.5 % and zirconium dioxide from 0.5 to 2 % are completely insoluble in a highly alkaline medium. Thus, this composition is the most optimal for use as a contrast agent in optical coherence tomography.

**Keywords:** Optical coherence tomography; contrast agents; nanomaterials; titanium dioxide;  $\text{SiO}_2$ ;  $\text{TiO}_2$ ;  $\text{ZrO}_2$ .

## 1. INTRODUCTION

Recently, research has proved the effective use of optical coherence tomography in such areas of clinical practice as gynecology, gastroenterology, urology, dermatology, ophthalmology, otolaryngology, dentistry, etc. [1-7]. Optical coherence tomography is a non-invasive method for visualizing the internal structure of optically inhomogeneous objects based on the principles of low-coherence interferometry using infrared light (0.75-1.3 microns) [2,8,9]. Optical coherence tomography allows us to study the internal microstructure of the body's integumentary tissues: skin and mucous membranes to a depth of up to 2 mm with a spatial resolution of 10-15 microns without violating the integrity of biological tissues [10-13]. At the same time, as a result of the optical heterogeneity of biological tissues, multiple scattering of probing radiation occurs, which significantly limits the depth of probing and the contrast of individual structures [14,15]. Currently, such techniques as soft tissue compression [16,17] and optical illumination are widely used to solve this problem. During optical illumination, substances are introduced into the biological tissue that reduce light scattering in the biological tissues as a result of matching the refractive indices of the structural elements of tissues and their environment. Such substances include some immersion liquids: glycerin, propylene glycol, concentrated glucose solutions, thanks to which optical illumination of biological tissues is achieved [2,18,19]. In addition to immersion liquids, nanoscale particles have recently been used to change the optical properties of biological tissues, for example: gold

nanowells, nanorods, nanocubes, as well as silver nanoparticles, titanium dioxide and others [20-26].

The use of contrasting nanoparticles leads to an amplification of the signal from internal inhomogeneities of biological tissues due to the scattering of probing radiation back [14,27,28]. In this paper, the contrasting properties of titanium dioxide nanoparticles in various compositions were considered.

## 2. MATERIALS AND METHODS

The main substances and reagents used in the work are shown in Table 1.

For the synthesis of  $\text{SiO}_2\text{-TiO}_2$ ,  $\text{SiO}_2\text{-ZrO}_2$ ,  $\text{TiO}_2\text{-ZrO}_2$  and  $\text{SiO}_2\text{-TiO}_2\text{-ZrO}_2$  nanocomposites, deionized water was used, which was obtained by passing distilled water through an Aquarius brand deionizer. The conductivity of the resulting water was 0.12 = 0.2 maxim.

The work also used alcohol-rectified brand "Extra" (TU 19P – 39 – 69). The content of ethyl alcohol is 96 %.

### 2.1 Method of Obtaining $\text{SiO}_2\text{-TiO}_2$ Nanocomposite

The developed method for obtaining  $\text{SiO}_2\text{-TiO}_2$  nanocomposite is a sol-gel process using tetraethoxysilane (TEOS) as a  $\text{SiO}_2$  precursor and titanium tetrachloride as a  $\text{TiO}_2$  precursor and an aqueous solution of aqueous solution of ammonia as a precipitator.

**Table 1. Substances and reagents used**

Substances and reagents	Purity class	Regulation
Ammonia aqueous, 25 %	Cleanforanalysis	GOST 3760 – 79
TEOS (tetraethoxycylane)	Extraclean	GOST 3475 – 75
Ethyl alcohol "Extra"	Cleanforanalysis	TU 19P – 39 – 69
Zirconyl nitrate 2-water	Cleanforanalysis	TU 6-09-1406-76
Titanium tetraisopropoxide	Clean	TU 2423-008-50284764-2006

The method of obtaining a  $SiO_2$ - $TiO_2$  nanocomposite includes the following stages:

- 1) At the first stage, TEOS and titanium tetrachloride are dissolved in an alcohol medium;
- 2) Then an aqueous solution of ammonia is introduced into the reaction mass;
- 3) Then the  $SiO_2$ - $TiO_2$  sol is mixed for 24 hours;
- 4) The resulting sols are concentrated and washed by centrifugation;
- 5) Then the samples are calcined at 500°C.

According to this method, a series of samples of  $SiO_2$ - $TiO_2$  nanocomposite containing from 10 to 90% titanium dioxide was made for further experiments.

## 2.2 Method of Obtaining $SiO_2$ - $ZrO_2$ Nanocomposite

The developed method for obtaining  $SiO_2$ - $ZrO_2$  nanocomposite is a sol-gel process using TEOS as a  $SiO_2$  precursor and zirconyl nitrate as a  $ZrO_2$  precursor and an aqueous solution of ammonia as a precipitator. The method of obtaining a  $SiO_2$ - $ZrO_2$  nanocomposite includes the following stages:

- 1) At the first stage, TEOS and zirconyl nitrate are dissolved in an alcohol medium;
- 2) Then an aqueous solution of ammonia is introduced into the reaction mass;
- 3) Then the  $SiO_2$ - $ZrO_2$  sol is mixed for 24 hours;
- 4) The resulting sols are concentrated and washed by centrifugation;
- 5) Then the samples are calcined at 500°C.

According to this method, a series of samples of  $SiO_2$ - $ZrO_2$  nanocomposite containing from 0.1 to 3% zirconium dioxide was made for further experiments.

## 2.3 Method of Obtaining a $TiO_2$ - $ZrO_2$ Nanocomposite

The developed method for producing the  $TiO_2$ - $ZrO_2$  nanocomposite is a sol-gel process using titanium tetrachloride as a precursor of  $TiO_2$  and zirconyl nitrate as a precursor of  $ZrO_2$  and an aqueous solution of ammonia as a precipitator. The essence of the technique is as follows: at the beginning, the initial substances of titanium tetrachloride and alcohol are mixed in a ratio of

1:10. Then, to form a  $Ti(OH)_4$  sol, a solution of zirconium nitrate and a 12.5% aqueous solution of ammonia is added drop by drop to the alcohol solution of  $TiCl_4$  to a neutral value of the active acidity of the medium pH = 6 – 7. To form a stable gel, the sol of the  $TiO_2$ - $ZrO_2$  nanocomposite is placed in a cool, dark place for 24 hours. The resulting gel is washed by centrifugation, and then dried at a temperature of 100 °C.

According to this method, a series of samples of  $TiO_2$ - $ZrO_2$  nanocomposite containing from 0.1 to 3% zirconium dioxide was made for further experiments.

## 2.4 Method of Obtaining $SiO_2$ - $TiO_2$ - $ZrO_2$ Nanocomposite

The developed method for obtaining  $SiO_2$ - $TiO_2$ - $ZrO_2$  nanocomposite is a sol-gel process. Tetraethoxysilane, titanium tetrachloride and zirconyl nitrate were used as starting materials. An aqueous solution of ammonia is used as a precipitator. Method of obtaining a nanocomposite  $SiO_2$ - $TiO_2$ - $ZrO_2$  includes the following stages:

- 1) At the first stage, tetraethoxysilane and titanium tetrachloride are dissolved in an alcoholic medium, and zirconyl nitrate is dissolved in distilled water;
- 2) Then the resulting solutions are mixed and an ammonia solution is introduced;
- 3) Then the  $SiO_2$ - $TiO_2$ - $ZrO_2$  sol is mixed for 24 hours;
- 4) The resulting sol is concentrated by centrifugation;
- 5) Next, the samples of the  $SiO_2$ - $TiO_2$ - $ZrO_2$  nanocomposite are calcined at 500°C.

According to this method, a series of samples of  $SiO_2$ - $TiO_2$ - $ZrO_2$  nanocomposite containing from 0.1 to 3% zirconium dioxide and from 7 to 10% titanium dioxide was made for further experiments.

## 2.5 Methods of Nanocomposites Research

### 2.5.1 X-ray phase analysis

The problem of studying the structure of matter is successfully solved with the help of a whole group of diffraction methods based on the scattering of X-rays by matter. The radiation source is an X-ray tube that provides an X-ray wavelength of 0.1 nm. X-rays are scattered by

the atoms of the sample and, folding up, form a diffraction pattern that can be recorded on a photographic film of a suitable format or use one or more X-ray detectors (counters) for this purpose [29].

By measuring the diffraction angles of the reflected rays, it is possible to determine the set of distances between the atomic planes using the appropriate formulas and to make a geometric model of the crystal lattice. The intensity of the rays reflected by each crystal system of planes is determined by the kind of atoms forming it and the nature of their location in the unit cell of the lattice.

For each material, a set of interplanar distances is obtained, comparing which with the tabular data of various substances, it is possible to determine the phase (substance) by their coincidence, or to isolate it in a mixture of other crystalline phases. The method makes it possible to control the value of interplane distances with an accuracy of  $\sim 10^{-5}$  nm and higher, as well as to trace the change in  $d$  during alloying, heat treatment, deformation and other influences on the material [30].

### 2.5.2 Scanning Electron Microscopy

Scanning electron microscopy (SEM) is a method based on obtaining an image of an object using an electron beam, and is characterized by higher values of spatial resolution and depth compared to optical microscopy. SEM makes it possible to conduct chemical analysis based on the registration of the spectrum of X-ray radiation generated when the sample surface is irradiated with an electron beam. The increase in SEM can be up to  $2 \times 10^5$  times [30].

The following based modes can be implemented in SEM:

- The mode of observation of reflected electrons;
- Mode of absorbed electrons;
- The use of contrast in the induced current mode opens up great opportunities for studying the electrical activity of defects in semiconductors.

The detector of X-ray radiation that occurs when substances are bombarded with electrons is used in SEM for microanalysis of the composition

of various surface areas and inclusions of the second phase. The analysis of the characteristic X-ray radiation makes it possible to determine the elementary composition and the ratio of various components in the inclusions of the second phase [31].

## 3. RESULTS AND DISCUSSION

Polycomponent systems based on silicon, titanium and zirconium dioxides were obtained by the sol-gel method, by co-precipitation of components from water-alcohol solutions. The following precursors were used in the work: tetraethoxysilane (grade A), titanium tetraisopropylate, 2-water zirconyl nitrate. Water-alcohol solutions were prepared on the basis of ethyl alcohol of the "Extra" brand (GOST 51652-2000) and deionized water (GOST R 52501-2005). Precipitation of silicon, titanium and zirconium hydroxides was carried out with an aqueous solution of ammonia. The developed method for obtaining multicomponent systems based on silicon, titanium and zirconium dioxides consists of several stages. At the first stage, water-alcohol solutions of precursors were mixed. Then, to activate the hydrolysis process with constant stirring, a 12.5% ammonia solution was slowly introduced to a neutral value of the active acidity of the medium  $\text{pH} = 6-7$ . At the second stage, to form an aggregatively stable gel of a multicomponent oxide system, the samples were placed in a dark, cool place for 24 hours. At the third stage, the resulting gels were washed by centrifugation, and then dried at a temperature of 100 C.

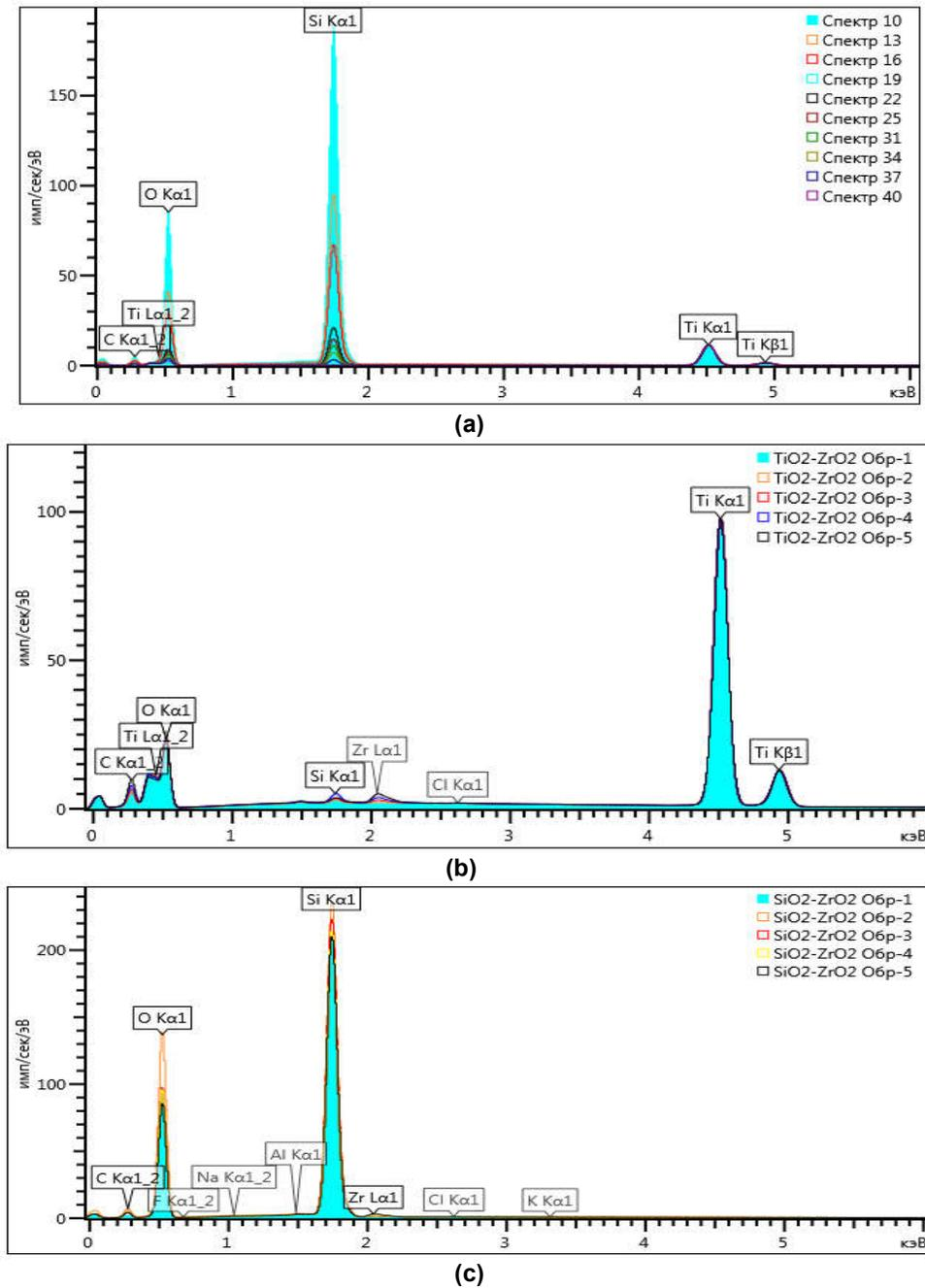
According to this method, 4 series of samples of multicomponent oxide systems were obtained. In the first series of  $\text{SiO}_2\text{-TiO}_2$  samples, the content of titanium dioxide was changed in the range from 10 to 90 % (wt.). In the second and third series of samples, the content of zirconium dioxide was changed in the range from 0.1 to 3 % (wt.), in the fourth series of samples, the content of titanium dioxide varied from 3 to 10 % (wt.), and zirconium dioxide from 0.1 to 3 % (wt.). The characteristics of multicomponent oxide systems are presented in Table 2. The mass content of silicon, titanium and zirconium dioxides, for convenience of comparison with the results of energy-dispersive X-ray diffraction analysis, is converted into atomic percentages of the corresponding elements.

Table 2. Elemental composition (theoretically calculated) of multicomponent oxide systems

Serial number	Type of multicomponent system	Sample no.	The content of the atoms of the elements. atom. %			
			Silicon	Titanium	Zirconium	Oxygen
1	SiO <sub>2</sub> -TiO <sub>2</sub>	1	30.76	2.57	–	66.67
		2	28.06	5.27	–	66.67
		3	25.21	8.12	–	66.67
		4	22.20	11.13	–	66.67
		5	19.1	14.23	–	66.67
		6	15.8	17.53	–	66.67
		7	12.13	21.20	–	66.67
		8	8.39	24.94	–	66.67
		9	4.28	29.05	–	66.67
		10	-	33.33	–	66.67
2	TiO <sub>2</sub> -ZrO <sub>2</sub>	1	–	33.31	0.02	66.67
		2	–	33.22	0.11	66.67
		3	–	33.11	0.22	66.67
		4	–	32.89	0.44	66.67
		5	–	32.67	0.66	66.67
3	SiO <sub>2</sub> -ZrO <sub>2</sub>	1	33.32	–	0.01	66.67
		2	33.25	–	0.08	66.67
		3	33.17	–	0.16	66.67
		4	33.00	–	0.33	66.67
		5	32.83	–	0.50	66.67
4	SiO <sub>2</sub> -TiO <sub>2</sub> -ZrO <sub>2</sub>	1	30.77	2.54	0.02	66.67
		2	30.80	2.45	0.08	66.67
		3	30.85	2.31	0.17	66.67
		4	30.93	2.07	0.33	66.67
		5	31.0	1.82	0.51	66.67

To study the microstructure of the samples and the local elemental composition, the method of scanning electron microscopy in combination with energy-dispersive X-ray diffraction analysis was used.

Figs. 1 and 2 show the EDS spectra of the samples of each series. Table 3 shows the elemental composition of all the studied samples.



**Fig. 1. EDS spectra of samples**

*a – the first series of samples  $\text{SiO}_2\text{-TiO}_2$  ( $w(\text{Ti})=2,57 - 33,33\%$ ), *b – the second series of samples  $\text{TiO}_2\text{-ZrO}_2$  ( $w(\text{Zr}) = 0.02 - 0.66\%$ ), *c – the third series of samples  $\text{SiO}_2\text{-ZrO}_2$  ( $w(\text{Zr}) = 0.01 - 0.5\%$***

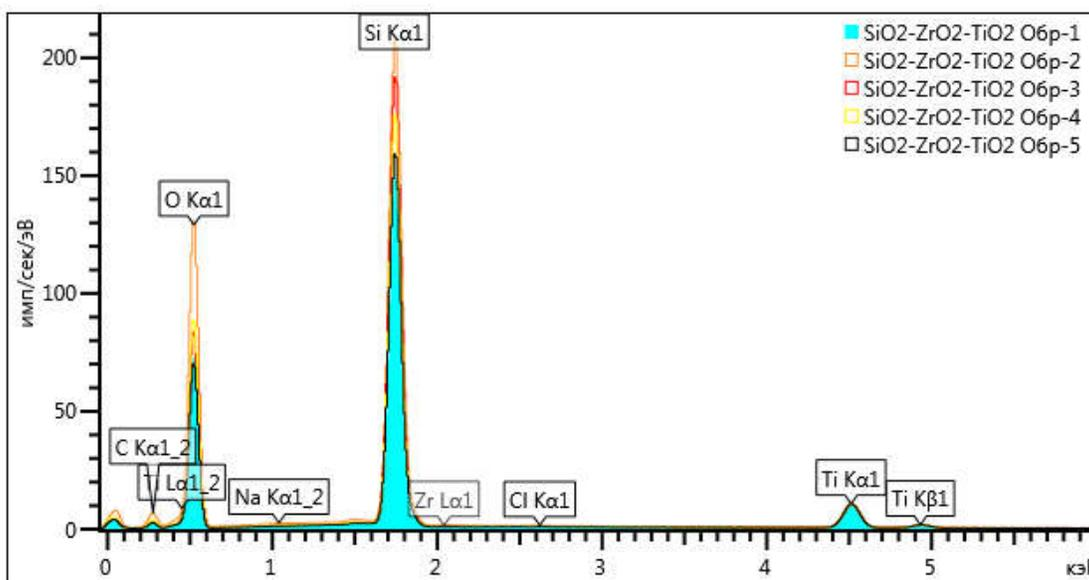


**Fig. 2. EDS-spectra of samples of a three-component oxide system  $\text{SiO}_2\text{-TiO}_2\text{-ZrO}_2$  ( $w(\text{Ti}) = 1,82 - 2,54 \%$ ;  $w(\text{Zr})=0.02 - 0.51 \%$ )**

A comparison of the theoretically calculated elemental composition of samples of polycapnent oxide systems (Table 2) and the one obtained on the basis of energy-dispersive X-ray diffraction analysis (Table 3) shows that after drying, there is a deviation from stoichiometry in the direction of increasing the

oxygen content in the samples. This suggests that the composition of multicomponent systems after drying, in addition to silicon, titanium and zirconium dioxides, includes complex oxo-, hydroxo and aqua complexes of the corresponding elements.

**Table 3. Local elemental composition of samples of polycapnent oxide systems after drying (experimental)**

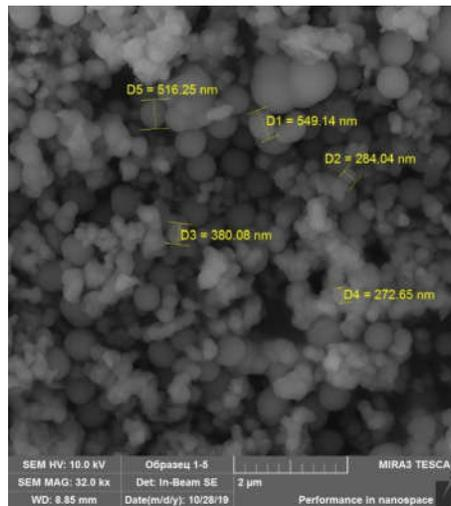
Serialnumber	Type of multi component system	The content of the atoms of the elements. atom. %			
		Silicon	Silicon	Silicon	Silicon
1	$\text{SiO}_2\text{-TiO}_2$	26.27	2.66	–	71.01
		23.78	4.64	–	71.58
		21.94	6.59	–	71.47
		18.52	9.41	–	72.07
		15.58	13.02	–	71.40
		12.75	15.39	–	71.86
		10.99	17.08	–	71.93
		8.01	19.12	–	72.87
		4.28	23.02	–	72.70
		–	28.40	–	71.60
2	$\text{TiO}_2\text{-ZrO}_2$	–	28.13	0.01	71.86
		–	28.57	0.05	71.38
		–	28.56	0.13	71.31
		–	27.89	0.28	71.83
		–	27.98	0.45	71.57
3	$\text{SiO}_2\text{-ZrO}_2$	30.19	–	0.01	69.80
		26.78	–	0.06	73.16
		30.81	–	0.12	69.07

Serialnumber	Typeofmulti component system	The content of the atoms of the elements. atom. %			
		Silicon	Silicon	Silicon	Silicon
4	SiO <sub>2</sub> -TiO <sub>2</sub> -ZrO <sub>2</sub>	30.09	–	0.21	69.70
		30.34	–	0.41	69.25
		24.67	2.69	0.01	72.63
		22.6	1.96	0.03	75.41
		27.02	2.58	0.06	70.34
		24.94	2.4	0.20	72.46
		26.08	2.83	0.30	70.79

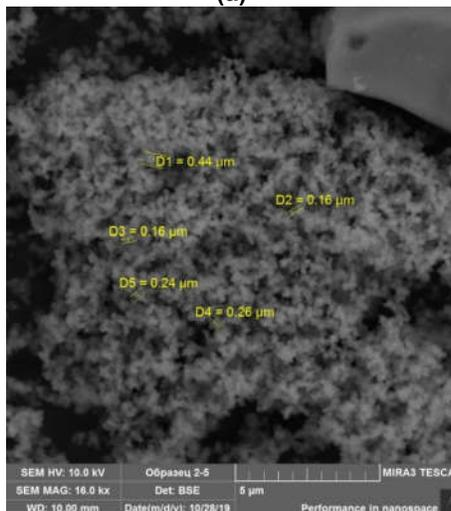
The results of a study of the microstructure of multicomponent oxide systems of different series obtained by scanning electron microscopy are shown in the figures SiO<sub>2</sub>-TiO<sub>2</sub> with a titanium dioxide content of 10 to 90 %; TiO<sub>2</sub>-ZrO<sub>2</sub> content of zirconium dioxide from 0.1 to 3 %; SiO<sub>2</sub>-ZrO<sub>2</sub>

content of zirconium dioxide from 0.1 to 3 %; SiO<sub>2</sub>-TiO<sub>2</sub>-ZrO<sub>2</sub> with a titanium dioxide content of 7 to 10% of zirconium dioxide from 0.1 to 3 %.

Photomicrographs of samples multicomponent systems SiO<sub>2</sub>-TiO<sub>2</sub> is presented in Fig. 3.



(a)



(b)

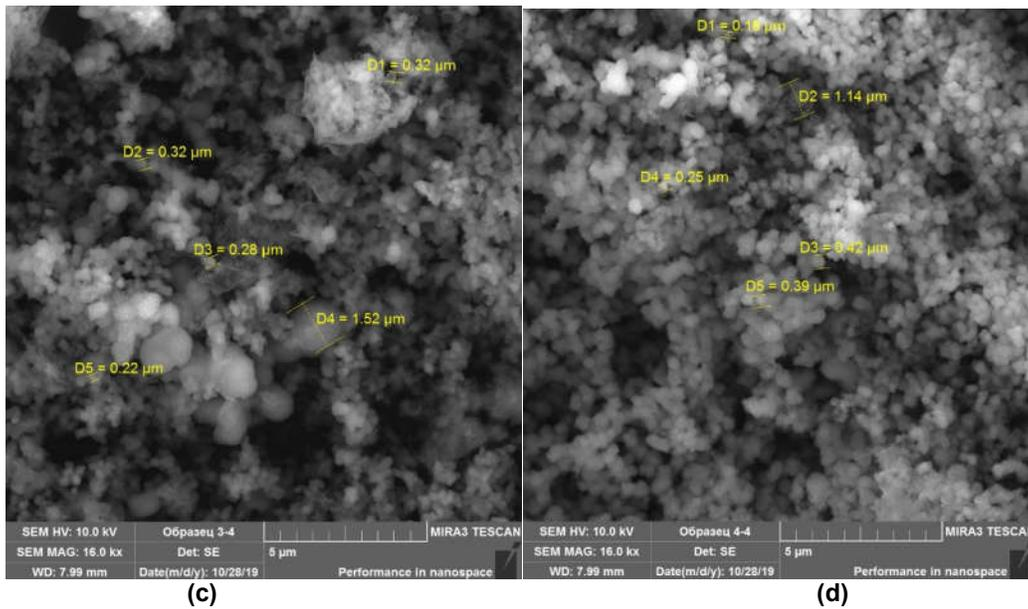
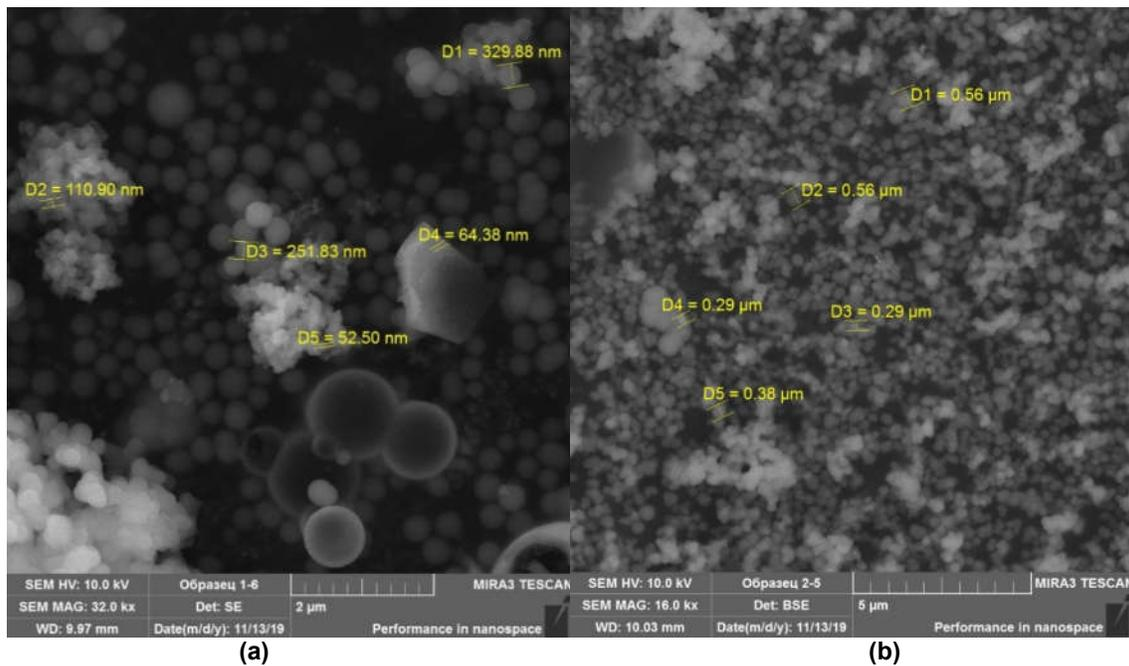


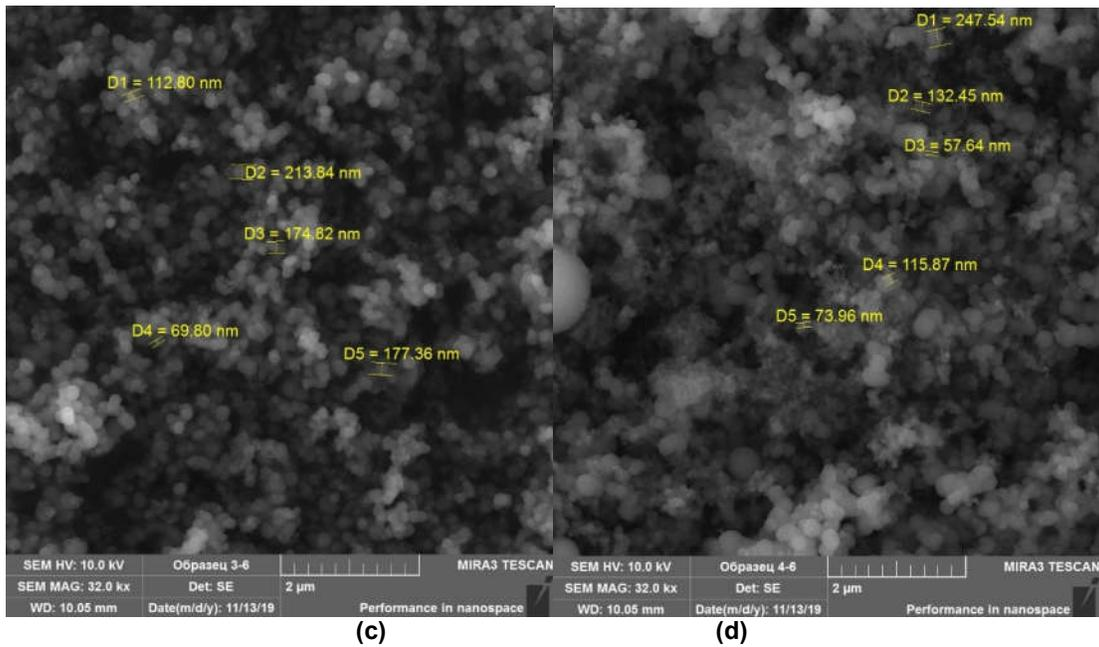
**Fig. 3. SEM micrographs of samples of the  $SiO_2-TiO_2$  polycrystalline oxide system**  
 a) 30.76% Si and 2.57% Ti, b) 28.06% Si and 5.27% Ti, c) 25.21% Si and 8.12% Ti, d) 22.20% Si and 11.13% Ti

The analysis of microphotographs showed that samples of the  $SiO_2-TiO_2$  multicomponent system containing from 2.57 at. % up to 8.12 at. % Ti, consist of spherical particles, that is, the shape and structure of the particles is determined by the component that is larger in the system. When the Ti content increases to 29.05 at. % the

structure of the samples changes – there is a transition from spherical particles to large aggregates of non-spherical shape.

Micrographs of samples of  $SiO_2-ZrO_2$  multicomponent systems are shown in Fig. 4.

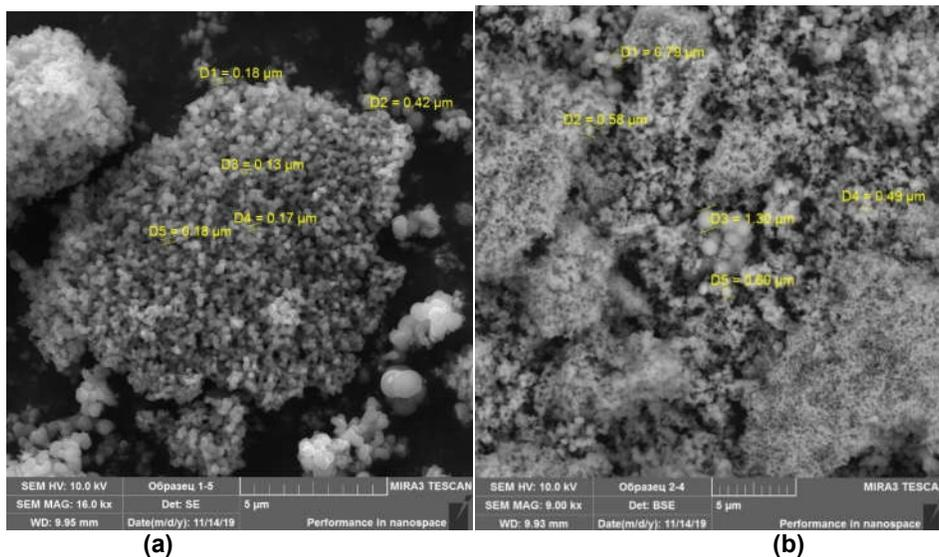




**Fig. 4. SEM-micrographs of  $\text{SiO}_2\text{-ZrO}_2$  samples 0.01% Zr (a), 0.08% (b) Zr, 0.17% Zr (c) and 0.33% (d) Zr**

The analysis of micrographs of the  $\text{SiO}_2\text{-ZrO}_2$  multicomponent system showed that the concentration of the introduced zirconium dioxide affects the microstructure of silicon dioxide. So when introducing 0.01 at. The addition of zirconium to the system leads to the formation of spherical particles with a diameter of 50 to 200 nm. An increase in the concentration of zirconium leads to a halving of the particle diameter. This may be due to the fact that zirconium compounds have solubility product

values significantly less than silicon compounds. When silicon and zirconium oxides are deposited together from water-alcohol solutions, zirconium compounds begin to crystallize first, which serve as crystallization centers for silicon oxide. The higher the initial concentration of zirconium in the solution, the more zirconium crystallization centers are formed in the system and the smaller the diameter of the polycomponent particles formed on their basis.



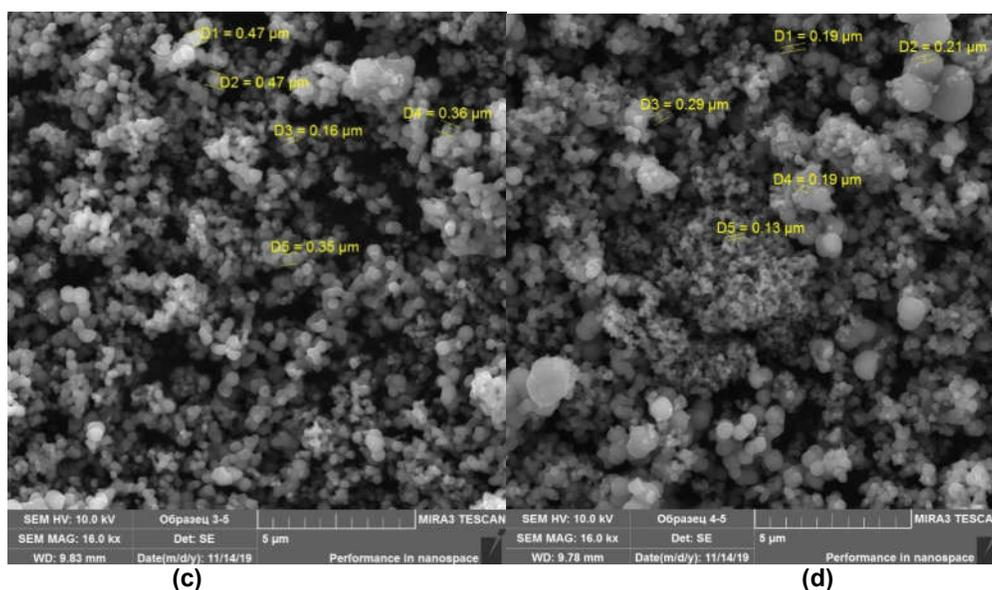


**Fig. 5. SEM-micrographs of  $TiO_2-ZrO_2$  samples**  
0.02% Zr (a), 0.11% (b) Zr, 0.44% Zr (c) and 0.66 % (d) Zr

Micrographs of the  $TiO_2-ZrO_2$  multicomponent system with different component contents are shown in Fig. 5.

Micrographs of samples of the  $TiO_2-ZrO_2$  series show that the structure of the multicomponent system is represented by large faceted aggregates of various shapes and spherical particles of smaller sizes. An analysis of the works of other authors showed that during the joint deposition of titanium and zirconium compounds from water-alcohol solutions, nucleation is the limiting stage of phase formation in the  $TiO_2-ZrO_2$  system [27,28,32]. The absence of germ-forming complexes affects both the structure and the size distribution of the resulting polycomponent particles. The process of joint deposition of titanium and zirconium compounds is complicated by the possibility of chemical interaction between them with the formation of complex salt systems. At a concentration of zirconium dioxide of 0.02 – 0.11 at.% these aggregates consist of nanoparticles with a diameter of 50-170 nm. It is important to note that an increase in the concentration of  $ZrO_2$  in a multicomponent system leads to an increase in the polydispersity of  $TiO_2-ZrO_2$  nanoparticles – the structure becomes more heterogeneous.

#### 4. CONCLUSION

As a result of the study of the microstructure of nanocomposites  $SiO_2-TiO_2$  It was found that samples containing from 10 % to 40%  $TiO_2$

consist of spherical particles, and when the  $TiO_2$  content increases from 40% to 90%, the structure of the samples changes: the formation of irregularly shaped particles occurs. The analysis of micrographs of the  $SiO_2-ZrO_2$  nanocomposite has established that at a concentration of 0.1%  $ZrO_2$ , the formation of spherical particles with a diameter of 200 to 1000 nm is observed. An increase in the concentration of  $ZrO_2$  to 2 % leads to the formation of two phases, the first with a diameter of nanocrystallites of the order of  $50 \text{ nm} \pm 10 \text{ nm}$  and the second from 100 to 500 nm. The microstructure of  $TiO_2-ZrO_2$  and  $SiO_2-TiO_2-ZrO_2$  nanocomposites is represented by aggregates of various shapes and sizes consisting of nanoparticles with diameters from 50-170 nm and from 50 to 1000 nm, respectively.

It was found that  $SiO_2-TiO_2-ZrO_2$  nanocomposites with a content of titanium dioxide from 8 to 9.5 % and zirconium dioxide from 0.5 to 2 % are completely insoluble in a highly alkaline medium. Thus, this composition is the most optimal for use as a contrast agent in optical coherence tomography.

#### CONSENT

It's not applicable.

#### ETHICAL APPROVAL

It's not applicable.

## COMPETING INTERESTS

Authors have declared that no competing interests exist.

## REFERENCES

- Baklanov I, Rodionova V, Ivashova V, Shvachkina L, Medvedeva V. Social Trends for Increasing Satisfaction with the Educational Services of a Modern University. *Quality-access to Success*. 2020;21(179):88-90.
- Nagdalian AA, Rzhepakovsky IV, Siddiqui SA, Piskov SI, Oboturova NP, Timchenko LD, Lodygin A, Blinov AV, Ibrahim SA. Analysis of the Content of Mechanically Separated Poultry Meat in Sausage Using Computing Microtomography. *Journal of Food Composition and Analysis*. 2021;100:103918
- Hite GJ, Mishvelov AE, Melchenko EA, Vlasov AA, Anfinogenova OI, Nuzhnaya CV, et al. Holodoctor Planning Software Real-Time Surgical Intervention. *Pharmacophore*. 2019;10(3):57-60
- Remizova AA, Dzgoeva MG, Tingaeva YI, Hubulov SA, Gutnov VM, Bitarov PA, et al. Tissue Dental Status and Features of Periodontal Microcirculation in Patients with New COVID-19 Coronavirus Infection.. *Pharmacophore*. 2021;12(2):6-13.  
Available:<https://doi.org/10.51847/5JlbnUbHkT>
- Razin MP, Minaev SV, Axelrov MA, Tarakanov VA, Svirsky AA, Trushin PV, Galanina AV, Barova NK, Gramsin AV, Smolentsev MM, Rakitina EN, Sklyar KE, Makhlin AM, Emelyanova VA, Sevkovsky IA. Diagnosis and treatment of the congenital diaphragmatic hernia in children: a multicenter research. *Medical News of North Caucasus*. 2019;14(2):302-308.  
DOI:  
<http://dx.doi.org/10.14300/mnnc.2019.14073> (In Russ.)
- Raevskaya AI, Belyalova AA, Shevchenko PP, Karpov SM, Mishvelov AE, Simonov AN et al. Cognitive Impairments in A Range of Somatic Diseases Diagnostics, Modern Approach to Therapy . *Pharmacophore*. 2020;11(1):136-41.
- Siddiqui, S.A.; Blinov, A.V.; Serov, A.V.; Gvozdenko, A.A.; Kravtsov, A.A.; Nagdalian, A.A.; Raffa VV, Maglaketidze DG, Blinova AA, Kobina AV, et al. Effect of Selenium Nanoparticles on Germination of Hordéum Vulgáre Barley Seeds. *Coatings*. 2021;11:862.  
Available:<https://doi.org/10.3390/coatings11070862>
- Gurenko SA, Sinelnikov BM, Nagdalian AA, Krivenko DV, Povetkin SN, Ziruk IV, et al. The Charge Components Proportions Influence On The Second Phase Emergence Probability, During Czochralski Process YAG MC Growth. *Res J Pharm BiolChem Sci*. 2018;9(1644):1644–7
- Yasnaya MA, Blinov AV, Blinova AA, Shevchenko IM, Maglaketidze DG, Senkova AO. Determination of optimal modes for measuring the size of colloidal particles by photon-correlation spectroscopy and acoustic spectroscopy. Physical and chemical aspects of the study of clusters nanostructures and nanomaterials. 2020;12:232-242.
- Minaev SV, Gerasimenko IN, Shchetinin EV, Schetinin V, Mishvelov AE, Nuzhnaya RV, Grigorova AN, Rubanova MF. 3D reconstruction in surgery of hydatid cyst of the liver. *Medical News of North Caucasus*. 2019;14(1.2):220-223.  
Available:<https://doi.org/10.14300/mnnc.2019.14019> (In Russ.)
- Oboturova NP, Evdokimov IA, Nagdalian AA, Kulikov YI, Gusevskaya OA. The study on the influence of the electrohydraulic effect on the diffusion coefficient and the penetration depth of salt into muscle tissues during salting. *Foods and Raw Materials*. 2015;3(2):74-81.
- Blinov AV, Siddiqui SA, Nagdalian AA, Blinova AA, Gvozdenko AA, Raffa VV, et al. Investigation of the influence of Zinc-containing compounds on the components of the colloidal phase of milk. *Arab J Chem*. 2021;14(7):103229.
- Cheboi PK, Siddiqui SA, Onyando J, Kiptum CK, Heinz V. Effect of Ploughing Techniques on Water Use and Yield of Rice in Maugo Small-Holder Irrigation Scheme, Kenya. *Agri Engineering*. 2021;3(1):110-7.  
DOI: 10.3390/agriengineering3010007.
- Demchenkov EL, Nagdalian AA, Budkevich RO, Oboturova NP, Okolelova AI. Usage of atomic force microscopy for detection of the damaging effect of CdCl<sub>2</sub> on red blood cells membrane. *Ecotoxicology and Environmental Safety*. 2021 ;208:111683.

15. Hight G Ya, Mishvelov AE, Nuzhnaya CV et al. New Image Modeling Features for Planning Surgical Interventions. *Research Journal of Pharmaceutical, Biological and Chemical Sciences*, 2019;10 (1):140-143.
16. Minaev SV, Kirgizov IV, Akselrov MA, Gerasimenko IN, Shamsiev JA., Bykov NI, Grigorova AN, Muravyev AV, Tussupkaliyev AB, Lukash Yu V., Muravyeva AA. Efficiency of retrieval bags for use during laparoscopic surgery to remove hydatid cysts of the liver. *Medical News of North Caucasus*. 2019;14(3):461-465.  
Available:<https://doi.org/10.14300/mnnc.2019.14111>
17. Magomedova UG, Khadartseva ZA, Grechko VV, Polivanova MN, Mishvelov AE, Povetkin SN, et al. The role of COVID-19 in the acute respiratory pathology formation in children, *Pharmacophore*. 2020;11(5):61-65.
18. Zimmerman T, Siddiqui SA, Bischoff W, Ibrahim SA. Tackling Airborne Virus Threats in the Food Industry: A Proactive Approach. *Int J Environ Res Public Health*. 2021;18(8):4335.  
DOI: 10.3390/ijerph18084335.
19. Ayivi R, Ibrahim S, Colleran H, Silva R, Williams L, Galanakis C, Fidan H, Tomovska J, Siddiqui SA. COVID-19: Human immune response and the influence of food ingredients and active compounds. *Bioactive Compounds in Health and Disease*. 2021;4(6):100.  
Available:<https://ffhdj.com/index.php/BioactiveCompounds/article/view/802>
20. Baklanov IS, Baklanova OA, Shmatko AA, Gubanova MA, Pokhilko AD. The Historical Past as a Factor of Sociocultural Transformations of Postmodernity. *Journal of History Culture and Art Research*. 2018;7(1):373-378.
21. Gurenko SA, Sinelnikov BM, Nagdalian AA, Povetkin, Sergey Nikolaevich Ziruk IV, Rodin IA, Oboturova NP, et al. A Strategy For Macrodefects Coordinates Detection In Oxide Monocrystals . *Res J Pharm BiolChem Sci*. 2018;9(1640):1640–3.
22. Blinov AV, Gvozdenko AA, Yasnaya MA, Blinova AA, Kravtsov AA, Krandievsky SO, Kramarenko VN. Synthesing and studying the structure of nanoscale copper (II) oxide stabilized by polyethylene glycol. *Herald of the Bauman Moscow State Technical University, Series Natural Sciences*. 2020;90:56-70.
23. Blinov AV, Gvozdenko AA, Kravtsov AA, Krandievsky SO, Blinova AA, Maglakelidze DG, Vakalov DS, Remizov DM, Golik AB. Synthesis of nanosized manganese methahydroxide stabilized by cysteine. *Materials Chemistry and Physics*. 2021;2651:124510.
24. Blinov AV, Gvozdenko AA, Yasnaya MA, Golik AB, Blinova AA, Shevchenko IM, Kramarenko VN. Effect of synthesis parameters on dimensional characteristics of Fe<sub>3</sub>O<sub>4</sub> nanoparticles: neural-network research. *Physical and chemical aspects of the study of clusters nanostructures and nanomaterials*. 2019;11:298-306.
25. Blinov AV, Kravtsov AA, Bondarenko EA, Bondarenko SA. Study of the influence of the type of the alcohol environment on the structure of nanoscale Zinc Oxide. *International Journal of Pharmacy and Technology*. 2016; 8(4):27129-27135.
26. Mishununa VV, Chapanov MM, Gakaeva KI, Tsoroeva MB, Kazanova SA, Gorlova MI, et al. Computed Quantum Chemical Modeling of the Effect of Nanosilver on Coronavirus COVID-19. *Pharmacophore*. 2021;12(2):14-21.  
Available:<https://doi.org/10.51847/LcTdy7pSqE>
27. Lunin LS, Lunina ML, Kravtsov AA, Sysoev IA, Blinov AV, Pashchenko AS. Effect of the Ag Nanoparticle Concentration in TiO<sub>2</sub>-Ag Functional Coatings on the Characteristics of GaInP/GaAs/Ge Photoconverters. *Semiconductors*. 2018;52(8):993-996.
28. Gvozdenko AA, Blinov AV, Yasnaya MA, Golik AB, Raffa VV, Kramarenko VN, Maglakelidze DG, Shevchenko IM. Computer quantum-chemical simulation of multicomponent SiO<sub>2</sub>-MexOy systems. *Physical and chemical aspects of the study of clusters nanostructures and nanomaterials*. 2020;12:394-404.
29. Siddiqui SA, Ahmad A. Implementation of Newton's algorithm using FORTRAN. *SN Comput Sci*. 2020;1(6):1-8.  
Available:<https://link.springer.com/article/10.1007/s42979-020-00360-3>  
[Accessed 18 Feb. 2021]
30. Siddiqui SA, Ahmad A. Implementation of Thin-Walled Approximation to Evaluate Properties of Complex Steel Sections Using C++. *SN Comput. Sci*. 2020;1(6):1-11.  
Available:<https://link.springer.com/article/10.1007/s42979-020-00354-1>

- [Accessed 18 Feb. 2021]
31. Bledzhyants GA, Mishvelov AE, Nuzhnaya KV, Anfinogenova OI, Isakova JA, Melkonyan RS. The Effectiveness of the Medical Decision-Making Support System "Electronic Clinical Pharmacologist" in the Management of Patients Therapeutic Profile, *Pharmacophore*. 2019;10(2):76-81.
32. Demir E, Turna F, Vales G, Kaya B, Creus A, Marcos R. In vivo genotoxicity assessment of titanium, zirconium and aluminium nanoparticles, and their microparticulated forms, in *Drosophila*. *Chemosphere*. 2013;93(10):2304-10. DOI:10.1016/j.chemosphere.2013.08.022

---

© 2021 Kupriyanov et al.; This is an Open Access article distributed under the terms of the Creative Commons Attribution License (<http://creativecommons.org/licenses/by/4.0>), which permits unrestricted use, distribution, and reproduction in any medium, provided the original work is properly cited.

*Peer-review history:*  
*The peer review history for this paper can be accessed here:*  
<https://www.sdiarticle4.com/review-history/71918>